

Direct and indirect constraints on isospin-violating dark matter

Yu-Feng Zhou

*State Key Laboratory of Theoretical Physics,
Kavli Institute for Theoretical Physics China,
Institute of Theoretical Physics, Chinese Academy of Sciences,
Beijing, 100190, P.R. China*

Abstract

The scenario of isospin-violating dark matter (IVDM) with destructive interference between DM-proton and DM-neutron scatterings provides a potential possibility to reconcile the experimental results of DAMA, CoGeNT and XENON. We explore the constraints on the IVDM from other direct detection experiments such as CRESST and SIMPLE, etc. and from the indirect DM searches such as the antiproton flux measured by BESS-Polar II. The results show that the relevant couplings in IVDM scenario are severely constrained.

Keywords: dark matter, isospin-violating interaction, cosmic-ray antiproton

Some of the recent dark matter (DM) direct detection experiments such as DAMA [1, 2, 3], CoGeNT [4, 5] and CRESST-II [6] have reported events which cannot be explained by conventional backgrounds. The excesses, if interpreted in terms of DM particle elastic scattering off target nuclei, may imply light DM particles with mass around 8–10 GeV and scattering cross section around 10^{-40} cm². Other experiments such as CDMS-II [7, 8], XENON10/100 [9, 10], and SIMPLE [11] etc., have reported null results in the same DM mass range.

A commonly adopted assumption on interpreting the DM direct detection data is that in spin-independent scatterings the DM particle couplings to proton (f_p) and to neutron (f_n) are nearly the same, i.e. $f_n \approx f_p$, which makes it straight forward to extract the DM-nucleon scattering cross sections. It is a good approximation for neutralino DM and DM models with Higgs portal, e.g. the scalar DM in left-right models [12, 13, 14, 15] and 4th generation Majorana neutrino DM [16]. However, in generic cases, the interactions may be isospin-violating [17, 18, 19, 20, 21, 22, 23]. In this scenario, the DM particle couples to proton and neutron with different strengths, possible destructive interference be-

tween the two couplings can weaken the bounds of XENON10/100 and move the signal regions of DAMA and CoGeNT to be closer to each other [21, 22]. In order to reconcile the data of DAMA, CoGeNT and XENON10/100, a large destructive interference corresponding to $f_n/f_p \approx -0.7$ is required [21].

Possible constraints on IVDM from the cosmic neutrinos and gamma ray on IVDM have been discussed previously in Refs. [24, 25, 26]. Recently the BESS-Polar II experiment has measured the antiproton flux in the energy range from 0.2 GeV to 3.5 GeV [27] which have higher precision compared with that from PAMELA [28] at low energies. In this talk, we discuss on the direct and indirect constraints on IVDM with focus on the cosmic-ray antiproton constraints. The details of our analysis can be found in Ref. [29].

For a DM particle χ elastically scattering off a target nucleus, the differential scattering cross section can be written as

$$\frac{d\sigma}{dE_R} = \frac{m_A F^2(E_R)}{2\mu_A^2 v^2} \sigma_0, \quad (1)$$

where $F(E_R)$ is the form factor of the nucleon and $\mu_A = (m_\chi m_A)/(m_\chi + m_A)$ is the DM-nucleus reduced

mass. The quantity σ_0 can be understood as the total scattering cross section at the limit of zero-momentum transfer which is related to $f_{p(n)}$ through

$$\sigma_0 = \frac{\mu_A^2}{\pi} [Zf_p + (A - Z)f_n]^2, \quad (2)$$

where Z is the atomic number and A is the atomic mass number. Under the assumption that the scattering is isospin conserving (IC), i.e., $f_n \approx f_p$, the total cross section σ_0 is independent of Z and only proportional to A^2 . One can define a cross section σ_p^{IC} which is the value of σ_p extracted from σ_0 under the assumption of IC interaction as

$$\sigma_p^{IC} \equiv \frac{\mu_p^2}{\mu_A^2 A^2} \sigma_0. \quad (3)$$

In the generic case where $f_n \neq f_p$, the true value of σ_p will differ from σ_p^{IC} by a factor $F(f_n/f_p)$ which depends on the ratio f_n/f_p and the target material

$$\sigma_p = F(f_n/f_p) \sigma_p^{IC}. \quad (4)$$

If the target material consists of N kind of relevant nuclei with atomic numbers Z_α ($\alpha = 1, \dots, N$) and fractional number abundances κ_α , and for each nucleus Z_α there exists M type of isotopes found in nature with atomic mass number $A_{\alpha i}$ and fractional number abundance $\eta_{\alpha i}$ ($i = 1, \dots, M$), the expression of $F(f_n/f_p)$ can be explicitly written as

$$F(f_n/f_p) = \frac{\sum_{\alpha,i} \kappa_\alpha \eta_{\alpha i} \mu_{A_{\alpha i}}^2 A_{\alpha i}^2}{\sum_{\alpha,i} \kappa_\alpha \eta_{\alpha i} \mu_{A_{\alpha i}}^2 [Z_\alpha + (A_{\alpha i} - Z_\alpha) f_n/f_p]^2}, \quad (5)$$

where $\mu_{A_{\alpha i}}$ is the reduced mass for the DM and the nucleus with atomic mass number $A_{\alpha i}$. For a given target material T , there is a particular value of f_n/f_p which corresponds to the maximal possible value of $F(f_n/f_p)$

$$\xi_T \equiv - \frac{\sum_{\alpha,i} \kappa_\alpha \eta_{\alpha i} \mu_{A_{\alpha i}}^2 (A_{\alpha i} - Z_\alpha) Z_\alpha}{\sum_{\alpha,i} \kappa_\alpha \eta_{\alpha i} \mu_{A_{\alpha i}}^2 (A_{\alpha i} - Z_\alpha)^2}. \quad (6)$$

The value of ξ_T varies with target material. In Tab. 1, we list the values of ξ_T for some typical material utilized by the current or future experiments.

If the ξ_T values of the target material used by two experiments are very close to each other, the tension between the two experimental results, if exists, is less affected by the effect of isospin violation. From Tab. 1 one finds that $\xi_{\text{Na}} \approx \xi_{\text{C}_2\text{ClF}_5} = -0.92$, $\xi_{\text{Xe}} \approx \xi_{\text{CsI}} \approx -0.7$ and $\xi_{\text{Si}} \approx \xi_{\text{Ca(W)O}_4} = -1.0$. Thus the tension between

DAMA signal from Na recoil and the upper bound from SIMPLE is unlikely to be alleviated by isospin violation, which can be clearly seen in Fig. 1. Similarly, if there exists contradictions between XENON and KIMS, CoGeNT and the Ar based experiments such as DarkSide, it can hardly be explained by isospin violating scattering. The SIMPLE result is also useful in comparing with the CRESST-II which utilizes Ca(W)O_4 which has $\xi_{\text{Ca(W)O}_4} = -1.0$. Obviously, for the experiments use the same target material, the possible tension between them cannot be relaxed by isospin violation, such as the tension between CoGeNT and CDMS-II, as both use germanium as target nucleus.

In Fig. 1, the allowed regions by the current experiments are shown in the (σ_p, m_χ) plane for $f_n/f_p = -0.70$. It can be seen that the overlapping region between GoGeNT and DAMA may still be consistent with the exclusion curve from the XENON100 2011 data [10]. However, If one considers the recently updated upper bounds from XENON100 [30], the main bulk of the overlapping region is excluded for both the GoGeNT results with and without surface event rejection corrections, which challenges the IVDM as a scenario to reconcile the results of DAMA, CoGeNT and XENON. The overlapping region between DAMA and CoGeNT seems also to be excluded by the results of SIMPLE [11] and CDMS-II independently [7, 8]. Note however that there still exists controversies regarding the detector stability of SIMPLE experiments [31, 32], the recoil energy calibration of CDMS experiment [33] and the extrapolation of the measured scintillation efficiency to lower recoil energy in the previous XENON100 data analysis [34, 35].

We assume that the DM particles interact with the SM light quarks through some heavy mediator particles much heavier than the DM particle such that both the scattering and the annihilation processes can be effectively described by a set of high dimensional contact operators

$$\mathcal{L} = \sum_{i,q} a_{iq} \mathcal{O}_{iq}. \quad (7)$$

If the DM particles are Dirac fermions, the relevant operators arising from scalar or pseudoscalar interactions are given by

$$\begin{aligned} \mathcal{O}_{1q} &= \bar{\chi} \chi \bar{q} q, \mathcal{O}_{2q} = \bar{\chi} \gamma^5 \chi \bar{q} q, \\ \mathcal{O}_{3q} &= \bar{\chi} \chi \bar{q} \gamma^5 q, \mathcal{O}_{4q} = \bar{\chi} \gamma^5 \chi \bar{q} \gamma^5 q. \end{aligned} \quad (8)$$

The operators from vector or axial-vector type interac-

	Xe	Ge	Si	Na(I)	Ca(W)O ₄	C ₂ ClF ₅	CsI	Ar
ξ_T	-0.70	-0.79	-1.0	-0.92(-0.73)	-1.0(-0.69)	-0.92	-0.71	-0.82

Table 1: Values of ξ_T for different target material. For NaI, the two values -0.92 and -0.73 correspond to the scattering off Na and NaI respectively. Similarly, for CaWO₄, the two values -1.0 and -0.69 corresponds to the scattering without and with tungsten nuclei respectively.

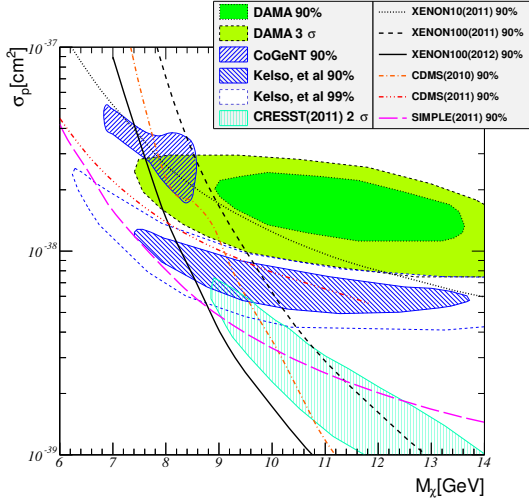


Figure 1: Favored regions and limits in the (σ_p, m_χ) plane from various experiments for $f_n/f_p = -0.70$ such as DAMA [2], GoGeNT unmodulated data [5], CoGeNT unmodulated data with surface event rejection factors taken from Kelso, et al [36], CRESST-II [6], XENON10/100 [9, 30], CDMS [7, 8] and SIMPLE [11].

tions are

$$\begin{aligned} O_{5q} &= \bar{\chi}\gamma^\mu\chi\bar{q}\gamma_\mu q, \quad O_{6q} = \bar{\chi}\gamma^\mu\gamma^5\chi\bar{q}\gamma_\mu q, \\ O_{7q} &= \bar{\chi}\gamma^\mu\chi\bar{q}\gamma_\mu\gamma^5 q, \quad O_{8q} = \bar{\chi}\gamma^\mu\gamma^5\chi\bar{q}\gamma_\mu\gamma^5 q, \end{aligned} \quad (9)$$

and the ones from the tensor interactions are

$$O_{9q} = \bar{\chi}\sigma^{\mu\nu}\chi\bar{q}\sigma_{\mu\nu}q, \quad O_{10q} = \bar{\chi}\sigma^{\mu\nu}\gamma^5\chi\bar{q}\sigma_{\mu\nu}q. \quad (10)$$

If the DM particles are Majorana particles the vector and tensor operators are vanishing identically. Among these operators only O_{1q} and O_{5q} contribute to spin-independent scattering cross sections at low velocities. The scattering cross sections induced by the operators O_{2q} and O_{6q} are velocity suppressed. The operators O_{7q} and O_{8q} contribute only to spin-dependent scattering cross section, and the nucleus matrix elements for the operators O_{3q} , O_{4q} , O_{9q} and O_{10q} are either vanishing or negligible. The DM annihilation into quarks through O_{1q} is a p -wave process, which is velocity suppressed. It does not contribute to the cosmic antiproton flux, but still contributes to the DM relic density as p -wave processes is non-negligible at freeze out.

Similarly, for DM being a complex scalar ϕ , possible operators are

$$\begin{aligned} O_{11} &= 2m_\phi(\phi^*\phi)\bar{q}q, \quad O_{12} = 2m_\phi(\phi^*\phi)\bar{q}\gamma^5q, \\ O_{13} &= (\phi^*\overleftrightarrow{\partial}_\mu\phi)\bar{q}\gamma^\mu q, \quad O_{14} = (\phi^*\overleftrightarrow{\partial}_\mu\phi)\bar{q}\gamma^\mu\gamma^5q \end{aligned} \quad (11)$$

Among those only O_{11} and O_{13} contribute to the spin-independent scatterings. The DM annihilations through operator O_{13} are p -wave processes.

In summary, we only consider four operators

$$O_{1q}, \quad O_{5q}, \quad O_{11q}, \quad \text{and} \quad O_{13q},$$

which are relevant to IVDM.

The DM couplings to nucleons $f_{p,n}$ can be expressed in terms of the DM couplings to quarks a_{iq} as follows

$$f_{p(n)} = \sum_q B_{iq}^{p(n)} a_{iq}. \quad (12)$$

For the Dirac DM with scalar interaction $a_{1q}\bar{\chi}\chi\bar{q}q$, one has $B_{1q}^{p(n)} = f_{Tq}^{p(n)} m_{p(n)}/m_q$ for $q = u, d, s$ and $B_{1q}^{p(n)} = (2/27)f_{TG}^{p(n)} m_{p(n)}/m_q$ for $q = c, b, t$, where $f_{Tq}^{p(n)}$ is the DM coupling to light quarks obtained from the σ -term $\langle N|m_q\bar{q}q|N \rangle = f_{Tq}^N M_N$, and $f_{TG}^{p(n)} = 1 - \sum_{q=u,d,s} f_{Tq}^{p(n)}$. In order to maximize the isospin violating effect, the coefficients $B_{1s,1c,1b,1t}^{p,n}$ must be strongly suppressed. Assuming that the DM-nucleon couplings are dominated by the DM couplings to the first generation quarks, the ratio f_n/f_p is given by

$$\frac{f_n}{f_p} \approx \frac{B_{1u}^n a_{1u} + B_{1d}^n a_{1d}}{B_{1u}^p a_{1u} + B_{1d}^p a_{1d}}. \quad (13)$$

The value of $f_n/f_p = -0.7$ can be translated into $a_{1d}/a_{1u} = -0.93$ at quark level. This value is the same for complex scalar DM. For operator O_{5q} one simply has $B_{5u}^{p(n)} = 2(1)$ and $B_{5d}^{p(n)} = 1(2)$, and $B_q^{p(n)} = 0$ for $q = c, s, t, b$.

$$\frac{f_n}{f_p} = \frac{a_{5u} + 2a_{5d}}{2a_{5u} + a_{5d}}. \quad (14)$$

Thus for $f_n/f_p = -0.7$, one finds $a_{5d}/a_{5u} = -0.89$.

Annihilation or decay of light DM particles in the galactic halo can contribute to exotic primary sources of the low energy cosmic ray antiprotons, which can

be probed or constrained by the current satellite- and balloon-borne experiments such as PAMELA and BESS-polar II, etc.. The predicted antiproton flux from DM annihilation depends on models of the cosmic-ray transportation, the distribution of Galactic gas, radiation field and magnetic field, etc.. It also depends on the particle and nuclear interaction cross sections. In this work, we use the numerical code GALPROP [37, 38, 39, 40, 41] which utilizes realistic astronomical information on the distribution of interstellar gas and other data as input and consider various kinds of data including primary and secondary nuclei, electrons and positrons, γ -rays, synchrotron and radiation etc. in a self-consistent way. In the GALPROP approach, we consider several diffusion models (parameter configurations). The different results between the models can be regarded as an estimate of theoretical uncertainties.

In the diffusion models of cosmic ray propagation, the Galactic halo where diffusion occurs is parameterized by a cylinder with half height Z_h and radius $R = 20 - 30$ kpc. The densities of cosmic ray particles are vanishing at the boundary of the halo. The processes of energy losses, reacceleration and annihilation take place in the Galactic disc. The source terms for the secondary cosmic rays are also confined within the disc. The diffusion equation for the cosmic ray particle is given by

$$\begin{aligned} \frac{\partial \psi}{\partial t} = & \nabla(D_{xx}\nabla\psi - \mathbf{V}_c\psi) + \frac{\partial}{\partial p}p^2D_{pp}\frac{\partial}{\partial p}\frac{1}{p^2}\psi \\ & - \frac{\partial}{\partial p}\left[\dot{p}\psi - \frac{p}{3}(\nabla \cdot \mathbf{V}_c)\psi\right] \\ & - \frac{1}{\tau_f}\psi - \frac{1}{\tau_r}\psi + q(\mathbf{r}, p), \end{aligned} \quad (15)$$

where $\psi(\mathbf{r}, p, t)$ is the number density per unit of total particle momentum which is related to the phase space density $f(\mathbf{r}, p, t)$ as $\psi(\mathbf{r}, p, t) = 4\pi p^2 f(\mathbf{r}, p, t)$. For steady-state diffusion, it is assumed that $\partial\psi/\partial t = 0$. The spatial diffusion coefficient D_{xx} is parameterized as

$$D_{xx} = \beta D_0 \left(\frac{\rho}{\rho_0}\right)^\delta, \quad (16)$$

where $\rho = p/(Ze)$ is the rigidity of cosmic ray particle and δ is the power spectral index which may take different values δ_1 or δ_2 when ρ is below or above the reference rigidity ρ_0 . D_0 is a normalization constant, and $\beta = v/c$ is the velocity of the cosmic ray particle. The convection term is related to the drift of antiproton from the Galactic disc due to the Galactic wind. The direction of the wind is usually assumed to be along the z -direction which is perpendicular to the galactic disc

and is a constant $\mathbf{V}_C = [2\theta(z) - 1]V_c$. The diffusion in momentum space is described by the reacceleration parameter D_{pp} which is related to the Alfvén speed V_a of the disturbances in the hydrodynamical plasma as

$$D_{pp} = \frac{4V_a^2 p^2}{3D_{xx}\delta(4 - \delta^2)(4 - \delta)w}, \quad (17)$$

where w stands for the level of turbulence which can be taken as $w = 1$ as D_{pp} depends only on the combination V_a^2/w . \dot{p} is related to the momentum loss rate, τ_f and τ_r are the time scale for fragmentation and radioactive decay respectively.

Thus the whole diffusion process depends on a number of parameters: $R, Z_h, \rho_0, D_0, \delta_1/\delta_2, V_c, V_a, \rho_s$ and γ_1/γ_2 . The recently updated analysis based on Markov Chain Monte Carlo fits to the astrophysical data show that Z_h should be around 4 – 7 kpc [42, 43]. In order to obtain a conservative upper bounds we choose $Z_h \approx 4$ kpc in our analysis.

We consider several typical propagation models in GALPROP, and focus on the models with the secondary antiproton background below the current data, which leaves room for DM contribution and results in conservative upper bounds. The first one is the plain diffusion model (referred to as “Plain”) in which there is no reacceleration term [41]. The second one is the conventional model (referred to as “Conventional”) with reacceleration included [39, 41]. The last one (referred to as “Global-Fit”) is the model from a global fit to the relevant astrophysical observables using Markov-Chain Monte Carlo method [43]. The main parameters of the three models are listed in Tab. 2.

The primary source term from the DM annihilation has the form

$$q(\mathbf{r}) = \eta n(\mathbf{r})^2 \langle \sigma v_{\text{rel}} \rangle \frac{dN}{dp}, \quad (18)$$

where $n(\mathbf{r}) = \rho(\mathbf{r})/m_\chi$, $\eta = 1/2(1/4)$ if the DM particle is (not) its own antiparticle and dN/dp is the injection spectrum per DM annihilation. For the DM profile we took the isothermal profile [44]

$$\rho(\mathbf{r}) = \rho_0 \left(\frac{r_\odot^2 + R_s^2}{r^2 + R_s^2} \right), \quad (19)$$

where $r_\odot = 8.5$ kpc is the distance of Solar system from the galactic center, $R_s = 2.8$ kpc and the local density is taken to be $\rho_0 = 0.3 \text{ GeV cm}^{-3}$. The choice of isothermal profile and the local density is again to achieve a conservative estimate of the antiproton flux, if the NFW profile is used, the predicted flux will be enhanced roughly by at most 70%, thus more severe constraints are expected.

model	$R(\text{kpc})$	$Z_h(\text{kpc})$	D_0	ρ_0	δ_1/δ_2	$V_a(\text{km/s})$	ρ_s	γ_1/γ_2
Plain	30	4.0	2.2	3	0/0.60	0	40	2.30/2.15
Conv.	20	4.0	5.75	4	0.34/0.34	36	9	1.82/2.36
Fit	20	3.9	6.59	4	0.3/0.3	39.2	10	1.91/2.40

Table 2: Propagation parameters in the “Plain” [41], “Conventional” [39, 41] and “Global-Fit” [43] models used in the GALPROP code. D_0 is in units of $10^{28} \text{cm}^2 \cdot \text{s}^{-1}$, the break rigidities ρ_0 and ρ_s are in units of GV.

In the case where the DM particles are thermal relics, possible large couplings to light quarks may under predict the DM relic abundance in comparison with the observed value $\Omega h^2 = 0.113 \pm 0.004$ [45]. Thus the relic density can also impose upper bounds on the relevant couplings. Whereas the p -wave annihilation processes give no contribution to the antiproton flux, in the calculation of DM relic density, the p -wave annihilation is nonnegligible as the typical relative velocity of DM particles is $v_{\text{rel}}/c \approx \mathcal{O}(0.3)$ at freeze out. The annihilation cross section times the relative velocity can be expressed as $\sigma v_{\text{rel}} = a + b v_{\text{rel}}^2$, where a and b are coefficients corresponding to the s -wave and p -wave contributions. For light DM around 10 GeV, $g_* = 61.75$, we find $x_f \approx 22$. The relic abundance is approximately given by

$$\Omega h^2 \simeq \frac{1.07 \times 10^9 \text{ GeV}^{-1}}{M_{pl}} \frac{x_f}{\sqrt{g_*}} \frac{1}{a + 3bx_f}. \quad (20)$$

We perform χ^2 analysis to obtain upper bounds on the DM isospin violating couplings to light quarks. For the sake of simplicity, we consider one operator at a time and ignore interference between the operators.

For the operators contribute to s -wave annihilation which leads to velocity-independent annihilation cross sections, the relevant DM couplings to quarks are found to be tightly constrained by both the cosmic antiproton flux and the thermal relic density. In Fig. 2 the constraints on the coefficients a_{5q} for operator $\mathcal{O}_{5q} = \bar{\chi} \gamma^\mu \chi \bar{q} \gamma_\mu q$ are shown in the $(a_{5u}, a_{5d}/a_{5u})$ plane. The mass of the Dirac DM particle is fixed at $m_\chi = 8 \text{ GeV}$. The results show that the DAMA- and CoGeNT-favored regions are in tension with both the cosmic antiproton flux and the thermal relic density.

At $a_{5d}/a_{5u} = -0.89$ which corresponds to $f_n/f_p = -0.70$, the DAMA and CoGeNT favored value is $a_{5u} \approx 1.6 \times 10^{-5} \text{ GeV}^{-2}$ corresponding to an annihilation cross section of $\langle \sigma v_{\text{rel}} \rangle \approx 3.4 \times 10^{-25} \text{ cm}^2$. As it can be seen in Fig. 3, for such a large cross section, the predicted antiproton flux is much higher than the current BESS-Polar II and PAMELA data and results in a huge $\chi^2/\text{d.o.f.} = 1.3 \times 10^6/35$ in the “Global-Fit” model and

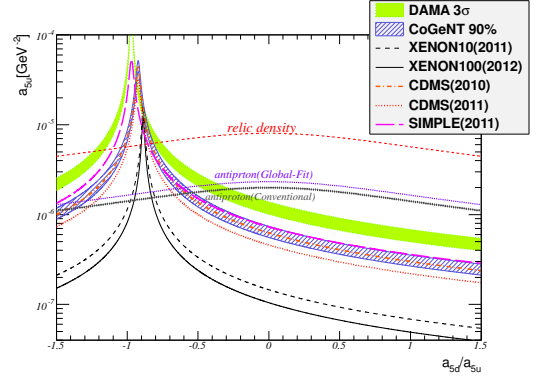


Figure 2: Upper bounds on the coefficient a_{5u} as a function of a_{5d}/a_{5u} at 95% CL from cosmic antiproton flux and DM relic density. The mass of DM particle is fixed at 8 GeV. The favored regions and exclusion contours from various experiments such as DAMA [2], CoGeNT [5], XENON [9, 30], CDMS [7, 8] and SIMPLE [11] are also shown.

an even larger one in the “Conventional” model. The upper bound set by the antiproton data at 95% CL is $a_{5u} \leq 1.7 \times 10^{-6} \text{ GeV}^{-2}$ in the “Global-Fit” model at $a_{5d}/a_{5u} = -0.89$, which is about an order of magnitude lower and corresponds to an annihilation cross section $\langle \sigma v_{\text{rel}} \rangle \approx 3.7 \times 10^{-27} \text{ cm}^2$. The predicted antiproton fluxes are also shown in Fig. 3. In the two propagation models, the upper bound from the “Conventional” model is slightly stronger than that from the “Global-Fit” model. In Fig. 3, we also plot the antiproton background of “Plain” model which is already higher than the data. Thus the upper bounds from this propagation model are expected to be much stronger. Since we are interested in conservative upper bounds, we do not further investigate the constraints in this model. In Fig. 3, the upper bound from the relic density is $a_{5u} \leq 6.0 \times 10^{-6} \text{ GeV}^{-2}$ at $a_{5d}/a_{5u} = -0.89$, which is weaker than that from the antiproton flux but still in tension with the DAMA- and CoGeNT-favored value.

Similar results are found for the operator \mathcal{O}_{11q} [29]. Compared with the case of \mathcal{O}_{5q} , the constraints on the coefficients of \mathcal{O}_{11q} are weaker, which is due to the fact that for the hadronic matrix element of scalar operator

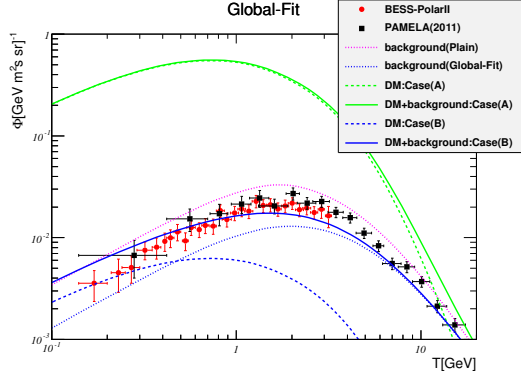


Figure 3: Predictions of cosmic antiproton spectra from DM annihilation induced by operator O_{5q} in the “Global-Fit” propagation model. Two cases are considered: (A) For $a_{5u} = 1.6 \times 10^{-5} \text{ GeV}^{-2}$ which is favored by the DAMA and CoGeNT experiments. (B) For $a_{5u} = 1.7 \times 10^{-6} \text{ GeV}^{-2}$ which is the maximal value allowed by the cosmic antiproton data at 95% CL. The ratio a_{5d}/a_{5u} is fixed at -0.89 corresponding to $f_n/f_p = -0.70$ and the mass of DM particle is fixed at 8 GeV. The data of BESS-Polar II [27] and PAMELA [28] are also shown; right) Same as left), but for the “Conventional” model.

$\bar{q}q$ the B_{iq} factors are larger than that for vector operator $\bar{q}\gamma^\mu q$, which allows smaller a_{iq} for the same value of $f_{p,n}$ and results in smaller annihilation cross sections. The constraint from the thermal relic density is in tension with the DAMA- and CoGeNT-favored values. The operators $O_{1q} = \bar{\chi}\chi\bar{q}q$ and $O_{13q} = (\phi^* \overleftrightarrow{\partial}_\mu \phi)\bar{q}\gamma^\mu q$ contribute to p -wave annihilation with cross section proportional to v_{rel}^2 . Thus they do contribute very little to the cosmic antiproton flux. However, their contributions to the thermal relic density cannot be neglected, as at freeze out the relative velocity is finite. For the operator O_{13q} one can see some tension between bounds set by the relic density and regions favored by DAMA and CoGeNT data. The constraint is not as stringent as that from the latest XENON100 data. For the operator O_{1q} , the constraints from relic density is rather weak. The difference is again due to the different B_{iq} factors for these two type of interactions.

It is straight forward to extend the discussions to Majorana fermions and real scalars. For the particles being its own antiparticles the primary source of the antiproton will be enhanced by a factor of 2 in Eq. (18), which may lead to more stringent constraints.

In summary, we have investigated the allowed values of DM-nucleon couplings in the scenario of IVDM for various target nuclei used in DM direct detections. We find that the recently updated XENON100 result excludes the main bulk of the overlapping signal region between DAMA and CoGeNT. We have shown that

whereas the effect of isospin violating scattering can relax the tensions between the data of DAMA, CoGeNT and XENON, the possible disagreement between some group of experiments such as that between DAMA and SIMPLE are not likely to be affected for any value of f_n/f_p . We have investigated the conservative constraints on the couplings between the IVDM and the SM light quarks from the recent cosmic ray antiproton data and that from the thermal relic density. Among the four operators relevant to IVDM O_{1q} , O_{5q} , O_{11q} , O_{13q} , the operators O_{5q} and O_{11q} are found to be tightly constrained by the antiproton data and O_{13q} is constrained by the relic density. Only the operator O_{1q} can survive both the constraints while contribute to large enough isospin violating interaction required by the current data of DAMA, CoGeNT and XENON.

This work is supported in part by the National Basic Research Program of China (973 Program) under Grants No. 2010CB833000; the National Nature Science Foundation of China (NSFC) under Grants No. 10975170, No. 10821504 and No. 10905084; and the Project of Knowledge Innovation Program (PKIP) of the Chinese Academy of Science.

References

- [1] R. Bernabei, et al., First results from DAMA/LIBRA and the combined results with DAMA/NaI, *Eur.Phys.J. C* 56 (2008) 333–355. [arXiv:0804.2741](#), doi:10.1140/epjc/s10052-008-0662-y.
- [2] C. Savage, G. Gelmini, P. Gondolo, K. Freese, Compatibility of DAMA/LIBRA dark matter detection with other searches, *JCAP* 0904 (2009) 010. [arXiv:0808.3607](#), doi:10.1088/1475-7516/2009/04/010.
- [3] R. Bernabei, et al., New results from DAMA/LIBRA, *Eur. Phys. J. C* 67 (2010) 39–49. [arXiv:1002.1028](#), doi:10.1140/epjc/s10052-010-1303-9.
- [4] C. E. Aalseth, et al., Results from a Search for Light-Mass Dark Matter with a P-type Point Contact Germanium Detector, *Phys. Rev. Lett.* 106 (2011) 131301. [arXiv:1002.4703](#), doi:10.1103/PhysRevLett.106.131301.
- [5] C. E. Aalseth, et al., Search for an Annual Modulation in a P-type Point Contact Germanium Dark Matter Detector, *Phys. Rev. Lett.* 107 (2011) 141301. [arXiv:1106.0650](#), doi:10.1103/PhysRevLett.107.141301.
- [6] G. Angloher, et al., Results from 730 kg days of the CRESST-II Dark Matter Search [arXiv:1109.0702](#).
- [7] D. S. Akerib, et al., Low-threshold analysis of CDMS shallow-site data, *Phys. Rev. D* 82 (2010) 122004. [arXiv:1010.4290](#), doi:10.1103/PhysRevD.82.122004.
- [8] Z. Ahmed, et al., Results from a Low-Energy Analysis of the CDMS II Germanium Data, *Phys. Rev. Lett.* 106 (2011) 131302. [arXiv:1011.2482](#), doi:10.1103/PhysRevLett.106.131302.
- [9] J. Angle, et al., A search for light dark matter in XENON10 data, *Phys. Rev. Lett.* 107 (2011) 051301. [arXiv:1104.3088](#), doi:10.1103/PhysRevLett.107.051301.

- [10] E. Aprile, et al., Dark Matter Results from 100 Live Days of XENON100 Data, *Phys. Rev. Lett.* 107 (2011) 131302. [arXiv:1104.2549](#), doi:10.1103/PhysRevLett.107.131302.
- [11] M. Felizardo, et al., Final Analysis and Results of the Phase II SIMPLE Dark Matter Search [arXiv:1106.3014](#).
- [12] W.-L. Guo, Y.-L. Wu, Y.-F. Zhou, Dark matter candidates in left-right symmetric models, *Int.J.Mod.Phys. D20* (2011) 1389–1397. doi:10.1142/S0218271811019578.
- [13] W.-L. Guo, Y.-L. Wu, Y.-F. Zhou, Searching for Dark Matter Signals in the Left-Right Symmetric Gauge Model with CP Symmetry, *Phys.Rev. D82* (2010) 095004. [arXiv:1008.4479](#), doi:10.1103/PhysRevD.82.095004.
- [14] W.-L. Guo, Y.-L. Wu, Y.-F. Zhou, Exploration of decaying dark matter in a left-right symmetric model, *Phys.Rev. D81* (2010) 075014. [arXiv:1001.0307](#), doi:10.1103/PhysRevD.81.075014.
- [15] W.-L. Guo, L.-M. Wang, Y.-L. Wu, Y.-F. Zhou, C. Zhuang, Gauge-singlet dark matter in a left-right symmetric model with spontaneous CP violation, *Phys.Rev. D79* (2009) 055015. [arXiv:0811.2556](#), doi:10.1103/PhysRevD.79.055015.
- [16] Y.-F. Zhou, Probing the fourth generation Majorana neutrino dark matter, *Phys.Rev. D85* (2012) 053005. [arXiv:1110.2930](#), doi:10.1103/PhysRevD.85.053005.
- [17] A. Kurylov, M. Kamionkowski, Generalized analysis of weakly-interacting massive particle searches, *Phys. Rev. D69* (2004) 063503. [arXiv:hep-ph/0307185](#), doi:10.1103/PhysRevD.69.063503.
- [18] F. Giuliani, Are direct search experiments sensitive to all spin-independent WIMP candidates?, *Phys. Rev. Lett.* 95 (2005) 101301. [arXiv:hep-ph/0504157](#), doi:10.1103/PhysRevLett.95.101301.
- [19] A. L. Fitzpatrick, D. Hooper, K. M. Zurek, Implications of CoGeNT and DAMA for Light WIMP Dark Matter, *Phys. Rev. D81* (2010) 115005. [arXiv:1003.0014](#), doi:10.1103/PhysRevD.81.115005.
- [20] S. Chang, J. Liu, A. Pierce, N. Weiner, I. Yavin, CoGeNT Interpretations, *JCAP* 1008 (2010) 018. [arXiv:1004.0697](#), doi:10.1088/1475-7516/2010/08/018.
- [21] J. L. Feng, J. Kumar, D. Marfatia, D. Sanford, Isospin-Violating Dark Matter, *Phys. Lett. B703* (2011) 124–127. [arXiv:1102.4331](#), doi:10.1016/j.physletb.2011.07.083.
- [22] M. T. Frandsen, et al., On the DAMA and CoGeNT Modulations, *Phys. Rev. D84* (2011) 041301. [arXiv:1105.3734](#), doi:10.1103/PhysRevD.84.041301.
- [23] X.-G. He, B. Ren, J. Tandean, Hints of Standard Model Higgs Boson at the LHC and Light Dark Matter Searches, *Phys.Rev. D85* (2012) 093019. [arXiv:1112.6364](#), doi:10.1103/PhysRevD.85.093019, doi:10.1103/PhysRevD.85.119902, doi:10.1103/PhysRevD.85.119906.
- [24] J. Kumar, J. G. Learned, M. Sakai, S. Smith, Dark Matter Detection With Electron Neutrinos in Liquid Scintillation Detectors, *Phys.Rev. D84* (2011) 036007. [arXiv:1103.3270](#), doi:10.1103/PhysRevD.84.036007.
- [25] S.-L. Chen, Y. Zhang, Isospin-Violating Dark Matter and Neutrinos From the Sun, *Phys.Rev. D84* (2011) 031301. [arXiv:1106.4044](#), doi:10.1103/PhysRevD.84.031301.
- [26] J. Kumar, D. Sanford, L. E. Strigari, New Constraints on Isospin-Violating Dark Matter, *Phys.Rev. D85* (2012) 081301. [arXiv:1112.4849](#).
- [27] K. Abe, et al., Measurement of the cosmic-ray antiproton spectrum at solar minimum with a long-duration balloon flight over Antarctica, *Phys. Rev. Lett.* 108 (2012) 051102. [arXiv:1107.6000](#), doi:10.1103/PhysRevLett.108.051102.
- [28] O. Adriani, et al., The cosmic-ray electron flux measured by the PAMELA experiment between 1 and 625 GeV, *Phys.Rev.Lett.* 106 (2011) 201101. [arXiv:1103.2880](#), doi:10.1103/PhysRevLett.106.201101.
- [29] H.-B. Jin, S. Miao, Y.-F. Zhou, Implications of the latest XENON100 and cosmic ray antiproton data for isospin violating dark matter [arXiv:1207.4408](#).
- [30] E. Aprile, et al., Dark Matter Results from 225 Live Days of XENON100 Data [arXiv:1207.5988](#).
- [31] J. Collar, Comments on 'Final Analysis and Results of the Phase II SIMPLE Dark Matter Search' [arXiv:1106.3559](#).
- [32] Reply to [arxiv:1106.3559](#) by J.I. Collar [arXiv:1107.1515](#).
- [33] J. Collar, A comparison between the low-energy spectra from CoGeNT and CDMS [arXiv:1103.3481](#).
- [34] J. Collar, D. McKinsey, Comments on 'First Dark Matter Results from the XENON100 Experiment' [arXiv:1005.0838](#).
- [35] Reply to the Comments on the XENON100 First Dark Matter Results [arXiv:1005.2615](#).
- [36] C. Kelso, D. Hooper, M. R. Buckley, Toward A Consistent Picture For CRESST, CoGeNT and DAMA, *Phys.Rev. D85* (2012) 043515. [arXiv:1110.5338](#), doi:10.1103/PhysRevD.85.043515.
- [37] A. Strong, I. Moskalenko, Propagation of cosmic-ray nucleons in the galaxy, *Astrophys.J.* 509 (1998) 212–228. [arXiv:astro-ph/9807150](#), doi:10.1086/306470.
- [38] I. V. Moskalenko, A. W. Strong, J. F. Ormes, M. S. Potgieter, Secondary anti-protons and propagation of cosmic rays in the galaxy and heliosphere, *Astrophys.J.* 565 (2002) 280–296. [arXiv:astro-ph/0106567](#), doi:10.1086/324402.
- [39] A. Strong, I. Moskalenko, Models for galactic cosmic ray propagation, *Adv.Space Res.* 27 (2001) 717–726. [arXiv:astro-ph/0101068](#), doi:10.1016/S0273-1177(01)00112-0.
- [40] I. V. Moskalenko, A. Strong, S. Mashnik, J. Ormes, Challenging cosmic ray propagation with antiprotons. Evidence for a fresh nuclei component?, *Astrophys.J.* 586 (2003) 1050–1066. [arXiv:astro-ph/0210480](#), doi:10.1086/367697.
- [41] V. Ptuskin, I. V. Moskalenko, F. Jones, A. Strong, V. Zirakashvili, Dissipation of magnetohydrodynamic waves on energetic particles: impact on interstellar turbulence and cosmic ray transport, *Astrophys.J.* 642 (2006) 902–916. [arXiv:astro-ph/0510335](#), doi:10.1086/501117.
- [42] A. Putze, L. Derome, D. Maurin, A Markov Chain Monte Carlo technique to sample transport and source parameters of Galactic cosmic rays: II. Results for the diffusion model combining B/C and radioactive nuclei, *Astron.Astrophys.* 516 (2010) A66. [arXiv:1001.0551](#).
- [43] R. Trotta, G. Johannesson, I. Moskalenko, T. Porter, R. R. de Austri, et al., Constraints on cosmic-ray propagation models from a global Bayesian analysis, *Astrophys.J.* 729 (2011) 106. [arXiv:1011.0037](#), doi:10.1088/0004-637X/729/2/106.
- [44] L. Bergstrom, P. Ullio, J. H. Buckley, Observability of gamma-rays from dark matter neutralino annihilations in the Milky Way halo, *Astropart.Phys.* 9 (1998) 137–162. [arXiv:astro-ph/9712318](#), doi:10.1016/S0927-6505(98)00015-2.
- [45] E. Komatsu, et al., Seven-Year Wilkinson Microwave Anisotropy Probe (WMAP) Observations: Cosmological Interpretation, *Astrophys.J.Suppl.* 192 (2011) 18. [arXiv:1001.4538](#), doi:10.1088/0067-0049/192/2/18.